LDPC-coded orbital angular momentum (OAM) modulation for free-space optical communication

Ivan B. Djordjevic,* and Murat Arabaci

Department of Electrical and Computer Engineering, University of Arizona, 1230 E. Speedway Blvd., Tucson, AZ 85721, USA
**ivan@ece.arizona.edu*

Abstract: An orbital angular momentum (OAM) based LDPC-coded modulation scheme suitable for use in FSO communication is proposed. We demonstrate that the proposed scheme can operate under strong atmospheric turbulence regime and enable 100 Gb/s optical transmission while employing 10 Gb/s components. Both binary and nonbinary LDPC-coded OAM modulations are studied. In addition to providing better BER performance, the nonbinary LDPC-coded modulation reduces overall decoder complexity and latency. The nonbinary LDPC-coded OAM modulation provides a net coding gain of 9.3 dB at the BER of 10^{-8}. The maximum-ratio combining scheme outperforms the corresponding equal-gain combining scheme by almost 2.5 dB.

OCIS codes: (060.2605) Free-space optical communication; (999.9999) Orbital angular momentum (OAM); (060.4080) Modulation; (999.9999) Forward error correction; (999.9999) Low-density parity-check (LDPC) codes; (010.1330) Atmospheric turbulence; (999.9999) Coded modulation.

References and links

1. H. G. Batshon, I. B. Djordjevic, and T. Schmidt, "Ultra high speed optical transmission using subcarrier-multiplexed four-dimensional LDPC-coded modulation," Opt. Express **18**(19), 20546–20551 (2010).
2. H. G. Batshon, I. B. Djordjevic, L. Xu, and T. Wang, "Modified hybrid subcarrier/amplitude/ phase/polarization LDPC-coded modulation for 400 Gb/s optical transmission and beyond," Opt. Express **18**(13), 14108–14113 (2010).
3. J. Leach, J. Courtial, K. Skeldon, S. M. Barnett, S. Franke-Arnold, and M. J. Padgett, "Interferometric methods to measure orbital and spin, or the total angular momentum of a single photon," Phys. Rev. Lett. **92**(1), 013601 (2004).
4. G. Gibson, J. Courtial, M. Padgett, M. Vasnetsov, V. Pas'ko, S. Barnett, and S. Franke-Arnold, "Free-space information transfer using light beams carrying orbital angular momentum," Opt. Express **12**(22), 5448–5456 (2004).
5. C. Paterson, "Atmospheric turbulence and orbital angular momentum of single photons for optical communication," Phys. Rev. Lett. **94**(15), 153901 (2005).
6. J. A. Anguita, M. A. Neifeld, and B. V. Vasic, "Turbulence-induced channel crosstalk in an orbital angular momentum-multiplexed free-space optical link," Appl. Opt. **47**(13), 2414–2429 (2008).
7. M. T. Gruneisen, W. A. Miller, R. C. Dymale, and A. M. Sweiti, "Holographic generation of complex fields with spatial light modulators: application to quantum key distribution," Appl. Opt. **47**(4), A32–A42 (2008).
8. S. Lin, and D. J. Costello, Jr., *Error Control Coding: Fundamentals and Applications* (Prentice Hall, 2004).
9. Z.-W. Li, L. Chen, L.-Q. Zeng, S. Lin, and W. Fong, "Efficient encoding of quasi-cyclic low-density parity-check codes," IEEE Trans. Commun. **54**(1), 71–81 (2006).
10. M. Arabaci, I. B. Djordjevic, R. Saunders, and R. M. Marcoccia, "Polarization-multiplexed rate-adaptive non-binary-quasi-cyclic-LDPC-coded multilevel modulation with coherent detection for optical transport networks," Opt. Express **18**(3), 1820–1832 (2010).
11. I. B. Djordjevic, "Adaptive modulation and coding for free-space optical channels," IEEE J. Opt. Com. Netw. **2**(5), 221–229 (2010).
12. L. C. Andrews, and R. L. Philips, *Laser Beam Propagation through Random Media* (SPIE Press, 2005).

1. Introduction

In order to satisfy high-bandwidth demands of future optical networks while keeping the system cost and power consumption reasonably low, we proposed the use of multidimensional coded modulation schemes in a series of articles [1,2]. The key idea behind this proposal was

#136548 - $15.00 USD Received 14 Oct 2010; revised 2 Nov 2010; accepted 3 Nov 2010; published 10 Nov 2010

to exploit various degrees of freedom already available for the conveyance of information on a photon such as frequency, time, phase, amplitude and polarization to improve the photon efficiency, while keeping the system cost reasonably low. On the other hand, it is well known that photons can carry both spin angular momentum (SAM) associated with polarization, and orbital angular momentum (OAM) associated with azimuthal phase of the complex electric field [3–5]. Each photon with azimuthal phase dependence of the form $\exp(l\phi\hbar)$ (l = 0, ± 1, ± 2,…) can carry an OAM of $l\hbar$. Because OAM eigenstates are orthogonal, in principle, an arbitrary number of bits per single photon can be transmitted. So far, the application of multiple photon degrees of freedom has mostly been related to the fiber-optics communication [1,2], and the OAM as a degree of freedom has not been studied. The ability to generate/analyze states with different OAMs by using interferometric or holographic methods [3–7] allows the realization of free-space optical (FSO) communication systems with ultra-high photon efficiencies, which are expressed in terms of number of bits per photon. The OAM modulation and multiplexing can, therefore, be used to solve the data rate incompatibility problem between FSO and fiber-optic links. The OAM multiplexing has been studied in [6] from an information theoretic point of view. Here we are concerned with *OAM modulation* instead. We propose a low-density parity-check (LDPC)-coded OAM modulation scheme that can operate under strong atmospheric turbulence and enable 100 Gb/s optical transmission while employing 10 Giga Symbols/s (GS/s) commercially available components.

Various applications of interest of OAM FSO systems include: (i) in cellular systems, to establish connection between mobile telephone switching office (MTSO) and base stations (BSs), (ii) in WiMax, to extend coverage and reliability by connecting WiMax BSs with OAM FSO links; (iii) in ultra wideband (UWB) communications, to extend wireless coverage range; (iv) in access networks, to increase data rate and reduce system cost and deployment time; (v) in ground-to-satellite/satellite-to-ground FSO communications to increase data rate; (vi) in intersatellite FSO communications and deep-space optical communications; and (vii) in aircraft-to-satellite/satellite-to-aircraft communications. The application to intersatellite and deep-space communications is of high importance since the atmospheric turbulence does not represent an issue.

The paper is organized as follows. The proposed binary and nonbinary LDPC-coded OAM modulation schemes are described in Section 2. The nonbinary quasi-cyclic LDPC codes suitable for use in combination with the proposed scheme are described in Section 3. The performance analysis is performed in Section 4. Finally, some important concluding remarks are provided in Section 5.

2. OAM based LDPC-coded FSO communication

In this section, we describe our approach to simultaneously increase the photon and spectral efficiencies based on multidimensional (N-dimensional) OAM coded modulation. $N = 2K + 1$ dimensions correspond to ($2K + 1$) OAM states (see Fig. 1(a)). By increasing the number of dimensions, i.e., the number of orthonormal basis functions, we can increase the aggregate data rate of the system while ensuring reliable transmission at these high transmission speeds by using LDPC codes at each level. The transmitter and receiver block diagrams are shown in Fig. 1. The $2K + 1$ independent data carrying TEM_{00} modes are shone on a series of volume holograms. Each volume hologram is programmed to one out of $2K + 1$ OAM modes with its corresponding diffraction angle properly adjusted so that a coaxial propagation of outgoing OAM beams is obtained. The resulting superposition beam is expanded by a telescope. During the propagation, the OAM superposition beam is affected by atmospheric turbulence. The FSO receiver link is designed based on the orthogonality of the Laguerre-Gaussian (LG) beams with different azimuthal mode numbers. At the receiver side, we use the same set of volume holograms to separate different OAM beams.

#136548 - $15.00 USD Received 14 Oct 2010; revised 2 Nov 2010; accepted 3 Nov 2010; published 10 Nov 2010

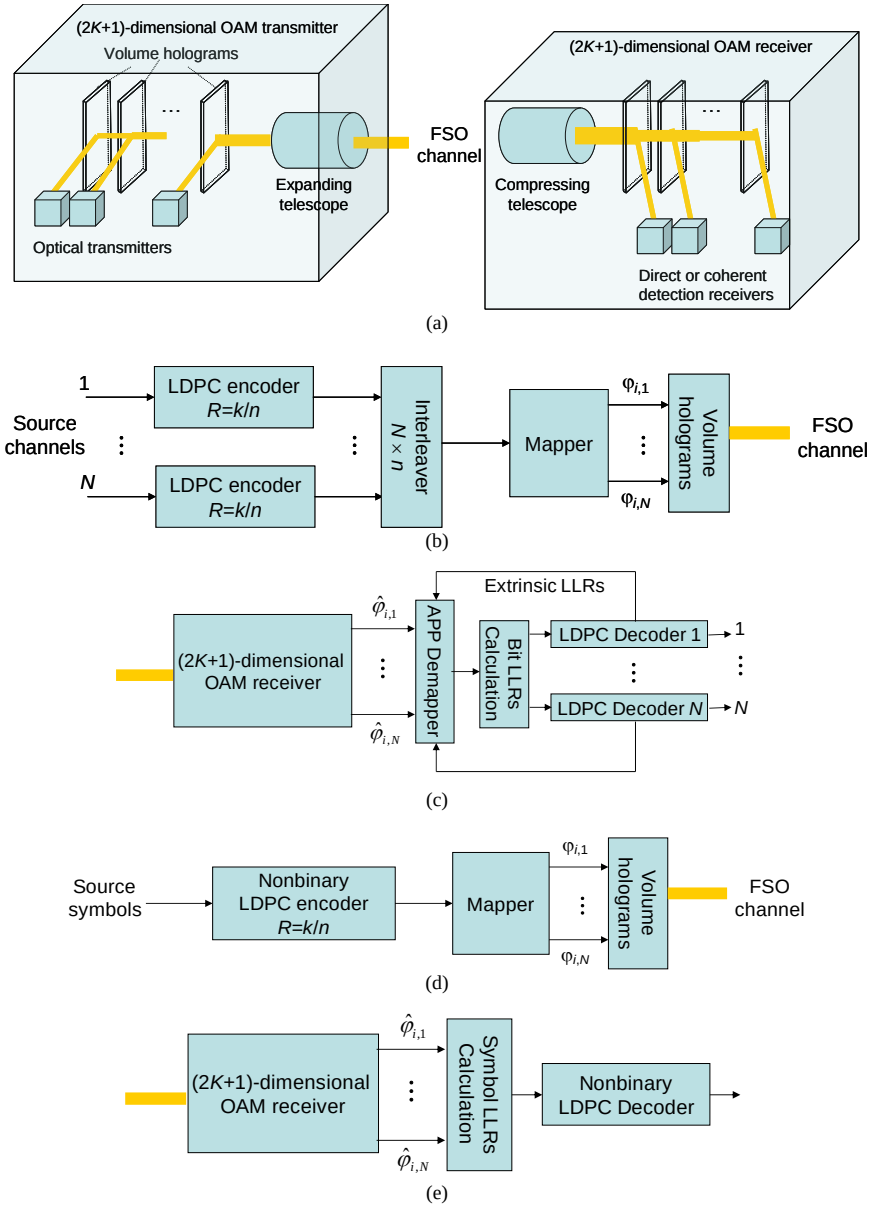

Fig. 1. Multidimensional LDPC-coded OAM modulation scheme: (a) OAM FSO system configuration; binary LDPC-coded (b) Tx and (c) Rx configurations; nonbinary LDPC-coded (d) Tx and (e) Rx configurations.

We present the transmitter and receiver configurations, when binary LDPC codes are used, in Fig. 1(b) and (c), respectively. As shown in the setup, N different bit streams coming from different information sources are encoded using identical binary LDPC codes. We refer to this LDPC-coded modulation scheme as the bit-interleaved LDPC-coded OAM modulation (BI-LDPC-OAM). The outputs of the encoders are interleaved by the ($N \times n$) block interleaver. The block interleaver accepts data from the encoders row-wise, and outputs the data column-wise to the mapper that accepts N bits at the time instance t. The mapper determines the corresponding M-ary ($M = 2^N$) signal constellation point by

#136548 - $15.00 USD Received 14 Oct 2010; revised 2 Nov 2010; accepted 3 Nov 2010; published 10 Nov 2010

$$s_i = C\sum_{j=1}^{N}\varphi_{i,j}\Phi_j, \quad (1)$$

as shown in Fig. 1(b), where C is a normalization factor. The mapping operation governed by Eq. (1) can be implemented as a look-up table (LUT) with N memory locations. Notice that only one LUT that operates at the symbol rate is needed. After mapping, the signals are modulated and sent over the FSO channel by an expanding telescope. In (1), which represents the general formula applicable to any N-dimensional constellation, the set $\{\Phi_1, \Phi_2,\ldots,\Phi_N\}$ represents a set of N orthogonal OAM basis functions. The number N is determined by the desired final rate. At the receiver side, after OAM demodulation and photodetection, see Fig. 1(a) and (c), the outputs of the N branches of the demodulator are sampled at the symbol rate and the corresponding samples are forwarded to an *a posteriori* probability (APP) demapper. The demapper provides the bit log-likelihood ratios (LLRs) required for the iterative LDPC decoding. From the description of the transmitter and the receiver setups, it is clear that the system is scalable to any number of dimensions. Scaling to higher dimensions comes only with a negligible penalty in terms of BER performance as long as the orthogonality of OAM states is preserved. In this paper, we will observe different signal constellation formats, such as: N = 1, 2, 3, 4, 8 and 10, where N is the number of OAM states. For N = 1 and 2, and $\varphi_{ij}\in\{-1,1\}$, the resulting constellations are similar to the conventional BPSK and QPSK, respectively, whereas for N = 3, the corresponding constellation is a cube. Note that for odd N, we do not use the central OAM mode for modulation; it can be used instead for beam positioning. To keep the system cost low, direct detection can be used. The simplest OAM modulation scheme with direct detection can be described by the following set of constellation points for N = 3: {(0,0,0), (0,0,1), (0,1,0), (0,1,1), (1,0,0), (1,0,1), (1,1,0), (1,1,1)}. (The normalization factor C in (1) is omitted to simplify presentation.) This modulation format can be straightforwardly extended to higher dimensions. Notice that we can use constellation points with larger amplitudes, but these constellation points will be affected more by atmospheric turbulence and also power efficiency will be reduced. In order to keep the system complexity low, we employ the simple modulation format described above and direct detection based on p.i.n. photodetector in transimpedance amplifier (TA) configuration. In this configuration, we need N external Mach-Zehnder modulators. Since optical amplifiers are not used at all, noise effects will be dominated by the TA. In the presence of atmospheric turbulence, the OAM states cannot preserve orthogonality to each other and thus OAM crosstalk occurs. OAM crosstalk can be modeled as a Gaussian noise process as shown in [6].

The corresponding transmitter and receiver configurations, when nonbinary LDPC codes are used, are shown in Fig. 1 (d) and (e), respectively. We refer to this coded-modulation scheme as the nonbinary-LDPC-coded OAM modulation (NB-LDPC-OAM) scheme. NB-LDPC-OAM offers several advantages over BI-LDPC-OAM: (1) N binary LDPC encoders/decoders needed for OAM modulation are collapsed into a single 2^N-ary encoder/decoder (reducing the overall computational complexity of the system), (2) the use of block (de-)interleavers; binary-to-non-binary and vice versa conversion interfaces are eliminated (reducing the complexity and latency in the system), and (3) the need for iterating extrinsic information between APP de-mapper and LDPC decoder is eliminated (reducing the latency in the system). In addition to these advantages, our simulations show that the NB-LDPC-OAM schemes provides higher coding gains than the corresponding BI-LDPC-OAM schemes.

Following this description of the proposed coded OAM modulation, in next section we describe a forward error correction scheme based on nonbinary LDPC codes, suitable for use in combination with OAM modulation.

3. Nonbinary quasi-cyclic LDPC codes

An LDPC code for which every cyclic shift of a codeword results in another codeword is commonly referred to as a quasi-cyclic LDPC (QC-LDPC) code [8]. The generator matrix of a q-ary QC-LDPC code can be represented as an array of circulant sub-matrices of the same

#136548 - $15.00 USD Received 14 Oct 2010; revised 2 Nov 2010; accepted 3 Nov 2010; published 10 Nov 2010

size over the finite field (Galois field) of q elements, GF(q). Therefore, QC-LDPC codes can be encoded in linear time using simple shift-register-based architectures [9]. The parity-check matrices of q-ary QC-LDPC codes can also be put in the form of an array of sparse circulant sub-matrices of equal size over GF(q) as shown in Eq. (2) below.

$$\mathbf{H} = \begin{bmatrix} \mathbf{H}_{0,0} & \mathbf{H}_{0,1} & \cdots & \mathbf{H}_{0,\rho-1} \\ \mathbf{H}_{1,0} & \mathbf{H}_{1,1} & \cdots & \mathbf{H}_{1,\rho-1} \\ \vdots & \vdots & \ddots & \vdots \\ \mathbf{H}_{\gamma-1,0} & \mathbf{H}_{\gamma-1,1} & \cdots & \mathbf{H}_{\gamma-1,\rho-1} \end{bmatrix}, \quad (2)$$

where $\mathbf{H}_{i,j}$, $0 \le i < \gamma$, $0 \le j < \rho$, is a circulant sub-matrix of $\mathbf{H}$. The modular structure of $\mathbf{H}$ presented in (2) can be exploited in hardware implementations of decoders for QC-LDPC codes to reduce routing complexity and hence silicon area consumption. In addition to their appealing structural advantages, QC-LDPC codes, when designed meticulously, perform as well as corresponding random LDPC codes [8]. These factors make QC-LDPC codes an important sub-class of LDPC codes and arguably the most encountered class of LDPC codes in practice. An efficient implementation of the generalized sum-product algorithm (QSPA) used for decoding q-ary LDPC codes employs the fast Fourier transform, which we refer to as FFT-QSPA. FFT-QSPA is particularly efficient over the non-binary fields whose order is a power of 2 since the complex arithmetic due to FFT can be avoided. In this paper, we use non-binary LDPC codes over the extension fields of the binary field, i.e. $q = 2^m$ for some positive integer m, to benefit from this nice property. Further details on FFT-QSPA and a reduced complexity variant of it can be found in [10] and references therein.

4. Performance evaluation

Figure 2(a) shows bit error rate (BER) performance results of the proposed BI-LDPC-OAM scheme as a function of the signal-to-noise-and-crosstalk ratio (SCNR) at the symbol rate of 10 GS/s for different N-dimensional (N-D) cases after 3 outer (APP demapper-LDPC decoder) iterations for two different LDPC codes of large girth g≥8. The number of inner (LDPC decoder) iterations was set to 25. In simulations, we use the model from [11]. To elaborate, it has been shown in [6] that OAM crosstalk distribution follows the Gaussian distribution, which motives the use of SCNR instead of signal-to-noise ratio (SNR) as a figure of merit, which is defined as

$$SCNR[\mathrm{dB}] = 10\log_{10}\left(\frac{E_b}{N_0+N_x}\right) = 10\log_{10}\left(\frac{E_b}{N_0}\frac{1}{1+\frac{N_x}{N_0}}\right) = SNR[\mathrm{dB}] - 10\log_{10}\left(1+\frac{N_x}{N_0}\right), \quad (3)$$

where E_b is the bit energy, N_0 is power spectral density (PSD) of noise and N_x is the PSD of OAM crosstalk. The OAM crosstalk is therefore included in our simulations by considering that a portion of the total noise power originates from OAM crosstalk, and there exists simple connection between SCNR and SNR (given by Eq. (3)). This allows us to make more general conclusions and to show the great potential of the proposed coded OAM modulation. In a practical implementation, we will need to measure the exact level of OAM crosstalk to determine the contributions of thermal noise and OAM crosstalk in the total noise power. If one wants to use SNR on x-axis and observe OAM crosstalk $\varepsilon_x = 10\log_{10}(N_x/N_0)$ as a parameter, the corresponding curves shown in Fig. 2 need to be shifted by $10\log_{10}\left(1+10^{\varepsilon_x/10}\right)$ dBs to the right. As shown in Fig. 2(a), the LDPC(16935,13550,0.80) code of column-weight 3 outperforms the shorter LDPC(8547,6922,0.81) code of column-weight 4 by 0.3 dB at the BER of 10^{-8} while achieving a net coding gain (NCG) of 9 dB at the same BER. The corresponding nonbinary LDPC(16935,13548) code outperforms the binary LDPC

#136548 - $15.00 USD Received 14 Oct 2010; revised 2 Nov 2010; accepted 3 Nov 2010; published 10 Nov 2010

code by 0.3 dB and provides an NCG of 9.3 dB at the same BER. The total aggregate rate can be calculated as $N \times 10$ Gb/s, and with $N = 10$, we achieve an aggregate data rate of 100 Gb/s. The proposed scheme is, therefore, compatible with future Ethernet technologies. To compensate for amplitude variations due to atmospheric turbulence, we perform the optimum power adaptation policy described in [11]. Namely, we estimate the FSO channel irradiance and transmit it back to the transmitter by using an RF feedback channel. We should note that since atmospheric turbulence changes slowly, with correlation time ranging from 10 μs to 10 ms, this is a plausible scenario for FSO channels with multi-Gb/s data rates. Therefore, since we transmit the channel state information back to transmitter, there is no need to use impractical long interleavers to deal with atmospheric turbulence.

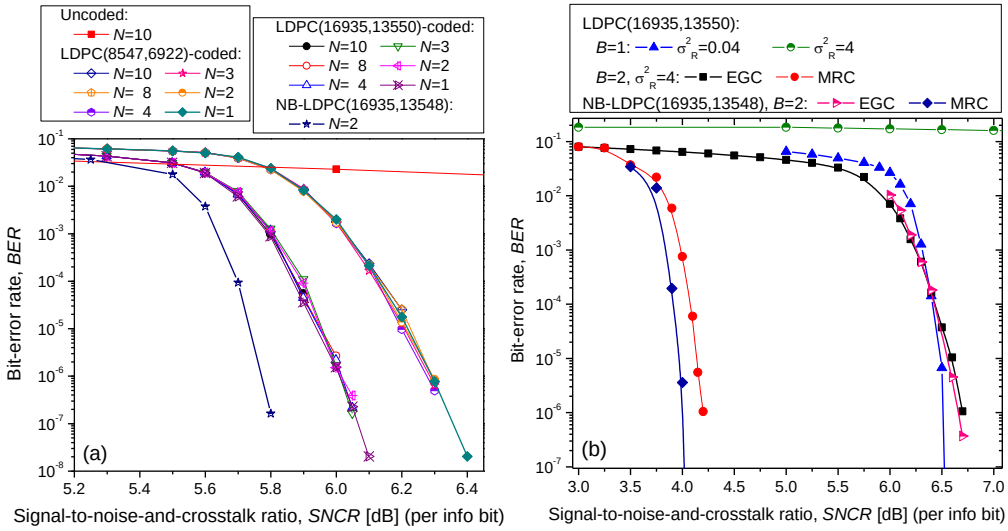

Fig. 2. (a) BER performance of (2K + 1)-dimensional LDPC coded OAM schemes for several different LDPC codes when adaptive power-loading is used in weak-turbulence regime. (b) BER performance of 10-D coded OAM modulation over FSO channel for receiver spatial diversity. *B* denotes the number of receiver diversity branches.

In Fig. 2(b), we provide BER results for the proposed LDPC-coded 10-D OAM modulation where the receiver spatial diversity is used to deal with amplitude variations due to atmospheric turbulence. Instead of the time-domain technique described above that requires the transmission of FSO irradiance back to the transmitter, we can use spatial-domain techniques to deal with atmospheric turbulence, namely, spatial-diversity. In the spatial-diversity based approach, an array of *B* direct detection receivers can be used to deal with this problem as explained in [11] (see Fig. 11.15 on pp. 466). Provided that the aperture diameter of each receiver is smaller than the spatial correlation width of the irradiance function, the array elements will be sufficiently separated so that they act independently. In that case, the summed output samples of the array will still be independent as shown in [11, pp. 469], and the need for deep interleavers is avoided. Spatial-diversity techniques are also suitable for dealing with the misalignment problem. By choosing an appropriate compressing telescope and using multiple OAM receivers in close proximity of each other, we can make sure that at least two OAM receivers are illuminated by a distant transmitter even in the presence of misalignment. Notice that the misalignment problem is a general problem present in any FSO system, and some conventional methods described in [11] are also applicable here. To characterize atmospheric turbulence, we can use Rytov variance σ_R^2 defined as follows [12]:

$$\sigma_R^2 = 1.23\ C_n^2\ k^{7/6} L^{11/6}, \tag{4}$$

where $k = 2\pi/\lambda$ (λ is the wavelength), L denotes the propagation distance, and C_n^2 is the refractive index structure parameter. The weak turbulence is associated with $\sigma_R^2 << 1$ while the

#136548 - $15.00 USD Received 14 Oct 2010; revised 2 Nov 2010; accepted 3 Nov 2010; published 10 Nov 2010

strong turbulence is with $\sigma_R^2>1$. In practice, the refractive index structure parameter C_2^n varies from 10^{-17} $m^{-2/3}$ (corresponding to the very weak turbulence regime) to 10^{-12} $m^{-2/3}$ (corresponding to the strong turbulence regime). For instance, the Rytov variance $\sigma_R^2 = 4$, corresponding to the strong turbulence regime, can be obtained with $C_n^2 = 2 \times 10^{-13}$ $m^{-2/3}$, $L = 1$ km, and $\lambda = 1550$ nm. On the other hand, the Rytov variance $\sigma_R^2 = 0.04$, corresponding to the weak turbulence regime, can be obtained with $C_n^2 = 2 \times 10^{-15}$ $m^{-2/3}$, $L = 1$ km, and $\lambda = 1550$ nm. From Fig. 2(b), we see that using two receivers is necessary to deal with the strong atmospheric turbulence. On the other hand, we can see that the weak turbulence regime does not require spatial diversity to be employed. Furthermore, in the weak turbulence regime, nonbinary LDPC codes are more effective than their binary counterparts. For the binary LDPC(16935,13550) code, the maximum ratio combining (MRC) approach outperforms the equal gain combining (EGC) approach by 2.46 dB at the BER of 10^{-9}. The nonbinary LDPC(16935,13548) code for MRC provides an additional 0.2 dB improvement.

In Fig. 3, we show the results of simulations for a deep-space link assuming that 64-pulse position modulation (PPM) is used in combination with 10 OAM modes, for different number of background photons n_b and different OAM crosstalk levels n_x. It is clear that imperfect OAM states can lead to a significant BER performance degradation. It is, therefore, essential to compensate for the OAM crosstalk introduced by imperfect OAM states generation and by atmospheric turbulence. In simulations, the Poisson channel is observed and the binary LDPC(15120,7560) code of girth 12 and column-weight 3 is used.

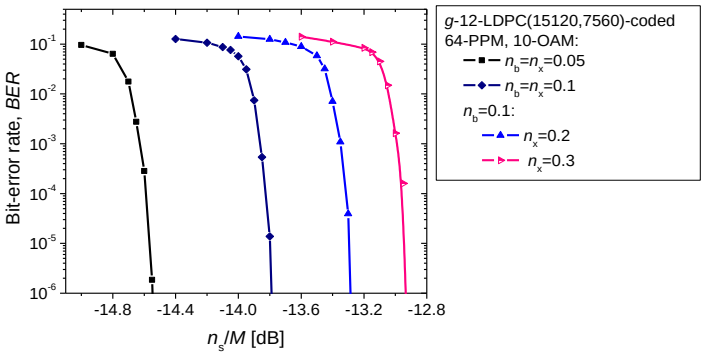

Fig. 3. BER performance of deep-space girth-12 LDPC-coded 10-OAM, 64-PPM system, where n_s denotes the number of signal photons and where $M = 64$.

5. Conclusion

We proposed LDPC-coded OAM modulation schemes capable of operating over the strong atmospheric turbulence regime and achieving 100 Gb/s optical transmission using 10 GS/s technology. The proposed scheme for $N = 10$, therefore, allows 10 bits/symbol transmission and represents an energy efficient scheme (because the coordinate values are restricted 0 or 1 values only). The proposed coded OAM modulation based FSO communication system can be used to: enable ultra-high-speed transmission to end-users, allow interoperability of various RF and optical technologies, reduce installation costs, reduce deployment time, and improve the energy efficiency of FSO communication links. Both binary and nonbinary LDPC-coded OAM modulations are studied. The nonbinary LDPC-coded OAM modulation outperforms the corresponding binary counterpart in terms of BER performance, and reduces decoder complexity as well as overall decoding latency.

Acknowledgments

This work was supported in part by the National Science Foundation (NSF) under Grants CCF-0952711 and ECCS-0725405.

#136548 - $15.00 USD Received 14 Oct 2010; revised 2 Nov 2010; accepted 3 Nov 2010; published 10 Nov 2010